Environ Earth Sci (2014) 71:1809–1820
DOI 10.1007/s12665-013-2585-7

ORIGINAL ARTICLE

Spatio-temporal variability in remotely sensed surface soil moisture and its relationship with precipitation and evapotranspiration during the growing season in the Loess Plateau, China

Xiaoying Li · Lichen Liu · Zhenghu Duan · Na Wang

Received: 28 January 2013 / Accepted: 27 May 2013 / Published online: 18 June 2013

Abstract The distribution and variability of surface soil moisture at regional scales is still poorly understood in the Loess Plateau of China. Spatial and temporal dynamics of surface soil moisture is important due to its impact on vegetation growth and its potential feedback to atmospheric and hydrologic processes. In this study, we analyzed surface soil moisture dynamics and the impacts of precipitation and evapotranspiration on surface soil moisture using remote sensing data during the growing season in 2011 for the Loess Plateau, which contain surface soil moisture, precipitation, vegetation index and evapotranspiration. Results indicate that the areas with low surface soil moisture are mainly located in the semi-arid region. Under dry surface soil moisture, evapotranspiration temporal persistence has a higher positive correlation (0.537) with surface soil moisture temporal persistence, and evapotranspiration is very sensitive to surface soil moisture. But under wet surface soil moisture regime, surface soil moisture temporal persistence has a higher negative correlation (−0.621) with evapotranspiration temporal persistence. Correlation of surface soil moisture and monthly precipitation, evapotranspiration and vegetation index illustrated that precipitation was a significant factor influencing surface soil moisture spatial variance. The correlation coefficients between monthly surface soil moisture and precipitation was varied in different climatic regions, which was 0.304 in arid, 0.364 in semi-arid, 0.490 in transitional and 0.300 in semi-humid regions. Surface soil moisture is more sensitive to precipitation, evapotranspiration, in transitional regions between dry and wet climates.

Keywords Surface soil moisture · SMOS · Loess Plateau · Remote sensing · Regional scale

X. Li (✉)
College of Resources and Environmental Sciences, Gansu Agricultural University, Lanzhou 730000, China
e-mail: lxy8211@163.com

X. Li · Z. Duan
Cold and Arid Regions Environmental and Engineering Research Institute, Chinese Academy of Sciences, Lanzhou 730000, China

L. Liu
College of Resource and Environmental Science, Lanzhou University, Lanzhou 730000, China

N. Wang
Shaanxi Provincial Meteorological Bureau, Xi'an 710014, China

Introduction

Soil moisture plays an important role in hydrological models, controlling the soil drainage and the surface runoff (Zakharova et al. 2012) and is the environmental variable synthesizing the effect of climate, soil and vegetation on the dynamics of water-limited ecosystems (D'Odorico et al. 2007). Surface soil moisture structure and evolution affect surface and subsurface runoff, land surface and atmosphere feedback, and groundwater recharge (Jacobs et al. 2004). Surface soil moisture plays a crucial role in hydrological and ecological processes at the land surface (Chen et al. 2010; Kimura and Shinoda 2012; Srivastava et al. 2012) and in the decision on the dynamic changes of the deep soil moisture (Mendez-Barroso et al. 2009; Vivoni et al. 2008; Wang et al. 2012b). Soil moisture dynamics are the central component of the hydrological cycle (Legates et al. 2011; Thakur et al. 2012a).

The Loess Plateau of China has a complex land surface environment (Li et al. 2012), the climate of which is a transitional zone between the southeastern humid monsoon climate and the northwestern continental dry climate (Wang et al. 2012b). Great attention has been paid to re-vegetation in previous soil conservation projects on the Loess Plateau (Zhou et al. 2013). An understanding of soil moisture heterogeneity across spatial scales has been considered to be critical to eco-hydrological research and particularly important for vegetation restoration in the semi-arid Loess Plateau of China (Yao et al. 2012). It is well possible that soil moisture can have large-scale or non-local impacts (e.g., by impacting large-scale circulation patterns); only few studies have investigated this topic until now (Seneviratne et al. 2010).

In the past studies, the spatial distribution of soil moisture and its correlations to other environmental factors in the Loess Plateau were studied most at a hillslope scale (Flores et al. 2009; Kim 2012; Zhu and Shao 2008) and a catchment scale (Wang et al. 2003; Yao et al. 2012; Zhu and Shao 2008). Geostatistics has been the most popular method to characterize the spatial patterns of soil moisture (Bi et al. 2009; Wang et al. 2001; Zhao and Shao 2010). At a regional scale, previous studies about soil moisture in the Loess Plateau have not been sufficient. One of the reasons is that measurements of soil moisture are rarely available at resolutions required to gain fuller insight into the interactions (Seneviratne et al. 2010). The direct linkage between hydrologic conditions and ecosystem responses has not been quantified, primarily due to a lack of regional observations (Mendez-Barroso et al. 2009). Developing observation capacities able to monitor the spatial and temporal variability of vegetation and soil moisture characteristics at a regional scale is needed for ecohydrology research (Wang et al. 2012a).

Satellite remote sensing has become an important tool for surface soil moisture monitoring. Remote sensing of soil moisture can be advantageous owing to its continuous temporal and spatial coverage (Legates et al. 2011). Passive microwave remote sensing has the capability to provide key elements of the terrestrial hydrological cycle such as surface soil moisture (Njoku and Li 1999). Microwave radiometry at low frequencies (L-band: 1.4 GHz, 21 cm) is an established technique for estimating surface soil moisture and sea surface salinity with a suitable sensitivity (Kerr et al. 2001). The Soil Moisture and Ocean Salinity (SMOS) mission is European Space Agency (ESA)'s second Earth Explorer Opportunity mission, launched in November 2009. SMOS carries a single payload, an L-Band 2-D interferometric radiometer in the 1,400–1,427 MHz protected band. This wavelength penetrates well through the atmosphere, and hence the instrument probes the earth surface emissivity. Surface emissivity can then be related to the moisture content in the first few centimeters of soil (Kerr et al. 2012). SMOS soil moisture products were rigorously validated and compared with the in situ data and retrievals data (Banks et al. 2012; Bircher et al. 2012; Gherboudj et al. 2012; Jackson et al. 2012; Sanchez et al. 2012; Zakharova et al. 2012). SMOS soil moisture products are able to detect temporal anomalies and the temporal evolution of ground soil moisture, though the soil moisture is slightly underestimated (Sanchez et al. 2012). The seasonal behavior of SMOS L2 products is generally in agreement with the in situ measurements in the Maqu (China) and Twente (The Netherlands) regions (Dente et al. 2012).

In this paper, our objectives were to (1) better understand the spatial variance of surface soil moisture on a regional scale, (2) characterize and compare the temporal distribution of surface soil moisture in different climatic regions on the Loess Plateau and (3) identify the relative importance of controlling factors for the temporal and spatial variability of surface soil moisture. The results would be beneficial to understand the causes of surface soil moisture changes of the Loess Plateau and enable the modeling of the regional water cycle and related eco-hydrological processes.

Study area and data

Study area

The Loess Plateau is located in the upper and middle reaches of the Yellow River with an average altitude of about 1,000 m above sea level, among the western Taihang Mountain, eastern Riyue–Helan Mountain, northern Qinling Mountain and southern Yinsan Mountain (from 100°54′ to 114°33′E and 33°43′ to 41°16′N). It covers a total area of 624,000 km^2 and has ancient deposits of thick loess (Shi and Shao 2000). The Loess Plateau is a subsystem of mutually interlinked and feedback system of northwest Gobi Desert, middle Loess Plateau and east alluvial plain (Bowler et al. 1987; Liu 1985.).

The Loess Plateau is one of the most environmentally sensitive regions in China (Zhang et al. 2006). As the most severe soil and water loss area in the world, over 60 % of the land in the Loess Plateau has been subjected to soil and water loss, with an average annual soil loss of 2,000–2,500 t/km^2 (Shi and Shao 2000).

Most land is arid or semi-arid (Zhang et al. 2006). The Loess Plateau belongs to the continental monsoon region with an annual mean temperature of 3.6–14 °C and annual precipitation ranging from 300 to 700 mm, both decreasing from southeast to northwest (He et al. 2004). The precipitation is concentrated during July to September due to the

effect of the East Asian monsoon (Zhang et al. 2009). The forest zones, forest-steppe, typical-steppe and desert-steppe distribute from southeast to northwest. The landscape of total plateau is much complicated with many ridges, Loess hills, ditches and ravines. Presently, the cropping area is $1{,}388.42 \times 10^4$ km^2, which is 29.4 %; the vegetable and orchard land area is 114.37×10^4 km^2, which is 2.4 %; the forest land area is $1{,}422.47 \times 10^4$ km^2, which is 30.1 %; and the grassland area is $1{,}802.49 \times 10^4$ km^2, which is 38.1 % (Zhou et al. 2013).

Field and remote sensing data sets

Ground-based data

We selected the growing season (June to November) in 2011 to validate satellite data and analyzed the relationships between precipitation, evapotranspiration and surface soil moisture. Ground-based monthly precipitation was obtained from a network formed by 217 rain gauge stations during 2011. The soil moisture observations were composed of eight soil moisture monitoring stations, distributed in the semi-arid and semi-humid areas on the Loess Plateau. At all stations, soil moisture was measured at 5-cm depth. To monitor the quality of the stations, independent handheld soil moisture measurements were conducted regularly (10 days). This study uses monthly soil moisture data at 5-cm depth which averaged from hourly observations of soil moisture over the 30-day intervals to match the SMOS compositing period during the study period. Figure 1 presents the locations of the stations.

SMOS L3 data

The ESA's SMOS mission, operating since November 2009, is the first satellite dedicated to measuring surface soil moisture (SSM) and ocean salinity. The SMOS level-3 monthly global product of the soil moisture product was used in this study. It provides a mean retrieved soil moisture weighted by their accuracy (DQX), vegetation optical thickness (separated for lower vegetation and forest) and RFI statistics over a month, without taking into account estimations affected by detected event (only frost for the moment) in the daily product (Berthon et al. 2012). The data were obtained from the Centre Aval de Traitement et des Données SMOS (CATDS) website (ftp://eftp.ifremer.fr/catds/cpdc). The spatial resolution of data is 0.26°.

Tropical rainfall measuring mission

Tropical rainfall measuring mission (TRMM) was launched on 27 November 1997 from the Tanegashima Space Center, Japan. The platform carries a dual complement of passive and active sensors, the TMI as passive and PR as active sensor to collect rain information (Islam et al. 2012). It orbits at an altitude of around 400 km with an inclination of 35° and an orbital period of around 92.5 min, completing approximately 16 orbits each day (Fleming et al. 2011). TRMM is the first meteorological satellite designed for quantitative estimation of tropical and subtropical rainfall (Xiong et al. 2009). The primary objective of TRMM is to measure rainfall and energy exchange over the tropical and subtropical regions of the world, in particular

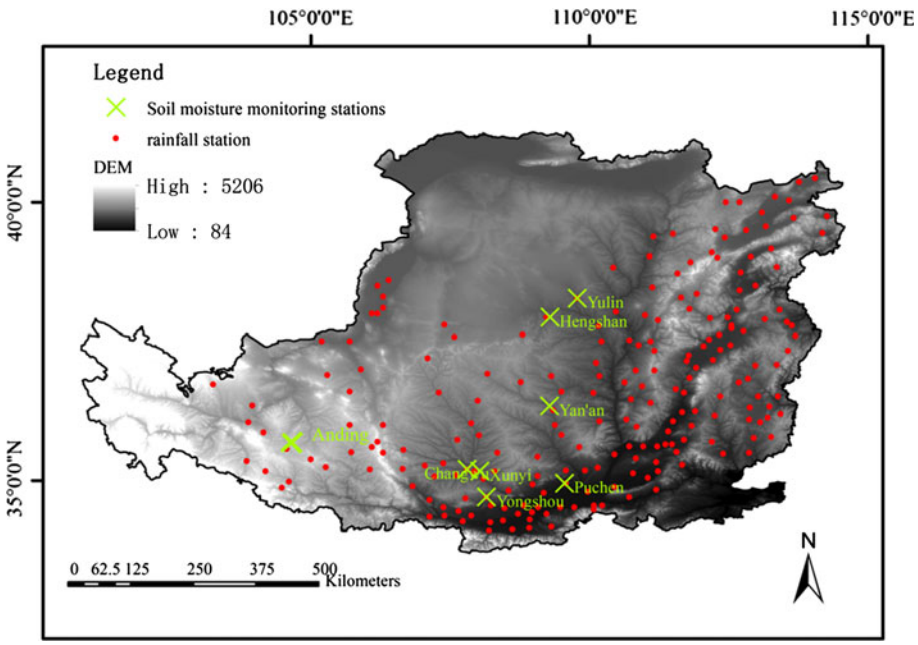

Fig. 1 Topography and the location of rain gauge and soil moisture stations in the Loess Plateau

covering the oceans and unsampled land areas (Kummerow et al. 1998, 2000).

The product used in this paper is the TRMM 3B43 (http://trmm.gsfc.nasa.gov/data_dir/). It is a time series of monthly average rainfall (in mm h^{-1}), inferred from data provided by multiple satellites in addition to TRMM, as well as rain gauge data provided by the Global Precipitation Climatological Center (GPCC, produced by the German Weather Service) and the Climate Assessment and Monitoring System (CAMS), produced by the National Oceanic Atmospheric Administration (NOAA) (Fleming et al. 2011). These gridded estimates have a calendar-month temporal resolution and a 0.25° × 0.25° spatial resolution (Jia et al. 2011). The version used in this work is number 6.

MODIS data

The MODIS data used in this paper are composed of Version-5 MODIS/Terra vegetation indices (NDVI) monthly level-3 global 1-km grid product (MOD13A3) and MODIS/Aqua evapotranspiration (ET) monthly global 1-km product (MOD16A2).

The monthly MODIS NDVI composites (MOD13A3) were obtained from the Land Processes Distributed Active Archive Center (LP DAAC) of NASA. MOD13A3 data are temporal averages of their 16-day versions. In addition to the quality control (QC) filter provided in the 16-day product, it uses a time-weighted average of the reflectance fields in the 16-day composited VI product that fall within a particular month and the ones that overlap in the beginning and end of each calendar month (Thakur et al. 2012b). The monthly product has a higher quality standard than the 16-day product (Anderson et al. 2010).

Products MOD16A2, which is the monthly ET (0.1 mm/month), were downloaded from MOD16 Global Terrestrial Evapotranspiration Data Set (ftp://ftp.ntsg.umt.edu/pub/MODIS/Mirror/MOD16/). The MOD16 ET data sets are estimated using Mu et al.'s improved ET algorithm (Mu et al. 2011) and has a temporal resolution of month at a spatial resolution of 1 km. MOD16 ET algorithm has a good performance in generating global ET data products, providing critical information on global terrestrial water and energy cycles and environmental changes (Mu et al. 2007, 2009, 2011). The correlation coefficients (CCs) of the MOD16 ET data with the ET measurements averaged over all the available days at the 46 flux tower sites was 0.86 (Mu et al. 2011), which means that the MOD16 ET data could be used in the analysis.

Each of the MODIS images was clipped, merged and reprojected using the MODIS reprojection tool. TRMM data and MODIS data were resampled to the 0.26° and 0.26° base resolution grids to match SMOS L3 surface soil moisture data sets.

Methods

Validation and statistical analysis

The monthly TRMM and SMOS L3 soil moisture satellite data have been validated based on the records from field stations. The determination coefficient (R^2) between the satellite data and the in situ data was computed from June to October.

Pearson's correlation coefficient between vegetation index, precipitation, evapotranspiration and surface soil moisture was calculated to explore the relationship between those factors.

Metrics of the spatial and temporal SSM dynamics

The concepts of the spatial and temporal persistence (Jacobs et al. 2004; Mendez-Barroso et al. 2009; Vivoni et al. 2008) were used to quantify the temporal and spatial variability of vegetation index (NDVI), precipitation, evapotranspiration and surface soil moisture. The spatial and temporal root mean square error (RMSE) of the mean relative difference (δ) for each image pixel is computed during the study period. The main difference between the spatial and temporal RMSE δ is the mean used to compute the relative difference (Mendez-Barroso et al. 2009).

Taking SMOS L3 data as an example, the analysis process of the temporal and spatial variability of SSM is as follows:

To get the spatial RMSE δ_s, we first calculated the spatial mean of SSM in the region for each SMOS L3 product as:

$$\overline{\mathbf{SSM}_{\mathrm{sp},t}} = \frac{1}{n}\sum_{s=1}^{n}\mathbf{SM}_{s,t} \quad (1)$$

where $\overline{\mathbf{SSM}_{\mathrm{sp},t}}$ is the spatial mean SSM for each month (t) over all pixels (s) and n is the total number of pixels; $\mathrm{SSM}_{s,t}$ is the SSM value for pixel (s) at time (t). Then, we obtained seven spatially averaged SSM values.

To compute the spatial RMSE δ_t, the temporal mean of EVI in each pixel is:

$$\overline{\mathbf{SSM}_{\mathrm{tm},s}} = \frac{1}{N_{\mathrm{t}}}\sum_{t=1}^{N_{\mathrm{t}}}\mathbf{SM}_{s,t} \quad (2)$$

where $\overline{\mathbf{SSM}_{\mathrm{tm},s}}$ is the temporal mean SSM and N_{t} is the total number of processed SMOS L3 images (7 in total).

The mean relative difference captures the difference between a pixel and the mean (spatial or temporal) for all

SMOS L3 images. The mean relative difference ($\overline{\delta}$) is computed as:

$$\overline{\delta} = \frac{1}{N_t}\sum_{t=1}^{N_t}\frac{\mathbf{SSM}_{s,t} - \overline{\mathbf{SSM}}^*}{\overline{\mathbf{SSM}}^*} \quad (3)$$

where $\overline{\mathbf{SSM}}^*$ is the spatial or temporal mean SSM, calculated by (1) or (2). The variance of the relative difference ($\sigma(\delta)^2$) is:

$$\sigma(\delta)^2 = \frac{1}{N_t - 1}\sum_{t=1}^{N_t}\left(\frac{\mathbf{SSM}_{s,t} - \overline{\mathbf{SSM}}^*}{\overline{\mathbf{SSM}}^*} - \overline{\delta}\right)^2 \quad (4)$$

Finally, the RMSE of the mean relative difference is defined as:

$$\mathbf{RMSE}\delta = \left(\overline{\delta}^2 + \sigma(\delta)^2\right)^{1/2} \quad (5)$$

The **RMSE** δ is a single metric used to classify time stability with respect to both bias and spread around the bias (Jacobs et al. 2004). Low values of RMSE δ_s indicate stable pixels that capture region-averaged conditions. This metric can track the temporal SSM dynamics for Loess Plateau. On the other hand, low RMSE δ_t indicates pixels with values close to the temporal mean and indicates pixels that have more limited seasonal changes at the site.

The temporal and spatial variability of precipitation, evapotranspiration and vegetation index were calculated in the same analysis process.

Results and discussion

Validation of TRMM and SSM

The TRMM 3B43 and SMOS L3 soil moisture data were extracted respectively by the location of stations and R^2 was calculated. Figure 2a presents the scatter diagram between monthly precipitation derived from TRMM 3B43 and in situ monthly precipitation. Based on the determination coefficient ($R^2 = 0.7347$) and scatter points slope methods, TRMM 3B43 data displayed good accuracy in the whole study area at monthly time scale.

Hengshan, Puchen and Yongshou stations located in no-data pixels, which did not have SMOS surface soil moisture data. Changwu station with high RFI was eliminated. The determination coefficient ($R^2 = 0.6458$) between SMOS SSM data and in situ data indicated moderate agreement between the two (Fig. 2b).

Figure 3 is the line chart between the SMOS L3 monthly soil moisture and the observed monthly soil moisture at the in situ station. The monthly behavior of SMOS L3 products is generally in agreement with the soil moisture behavior in the Yulin. Although the annual precipitation of these rain gauge stations was underestimated by SMOS L3 data, the SMOS L3 surface soil moisture effectively captured the trends in inter-month variability.

The results showed that TRMM 3B43 and SMOS L3 monthly data can be used to analyze the relationships between surface soil moisture, precipitation and evapotranspiration on the Loess Plateau.

Spatial distribution pattern of NDVI, precipitation, ET and SSM

Due to the East Asian monsoon, the amount of precipitation during the growing season decreases from southeast to northwest (Fig. 4a). Precipitation can reach a range from 800 to 1,000 mm in the southeastern part of the Loess Plateau, from 150 to 200 mm in the northwestern part and <100 mm in the desert. Based on precipitation isolines (precipitation from June to November in 2011), we divided the Loess Plateau into four climatic regions: arid ($P < 200$ mm), semi-arid (200 mm $< P <$ 400 mm), semi-humid 1 (400 mm $< P <$ 600 mm) and semi-humid 2 ($P > 600$ mm), where P is short for precipitation.

Similar to precipitation, the NDVI mean value during the growing season decreases gradually from southeast to northwest (Fig. 4b).

Figure 4c shows a map of the distribution of the mean value of ET during the growing season in the Loess Plateau. The mean value of ET in the southeast region is greater than in the northwest region. The smallest values were found in the desert, located in the northwest region.

The spatial distribution pattern of the mean value of SSM became more complex and showed great differences with the others. Figure 4d shows that the mean value of SSM during the growing season ranged from 0.04 to 0.21 $m^3\ m^{-3}$. The low value of SSM concentrated relatively in four areas: the loess hilly area of the Western Loess Plateau, the Mu Us Sandland, the hilly-gully region of the Northern Loess Plateau and typical-steppe, desert-steppe and steppe-desert zones in Southern Inner Mongolia on Loess Plateau. In those regions, rainfall and soil moisture can fatally influence vegetation production (Liu et al. 2011).

But Fig. 4 also shows that the value of NDVI, ET and SSM are higher in the most northern part of the Loess Plateau. Because the Inner-Mongolia reaches of Yellow River develops multi watercourses and has many river bends and shoals in this region, runoff is sensitive to surface soil moisture in this area. This situation led to higher SSM, better vegetation growth and more plant transpiration in this area.

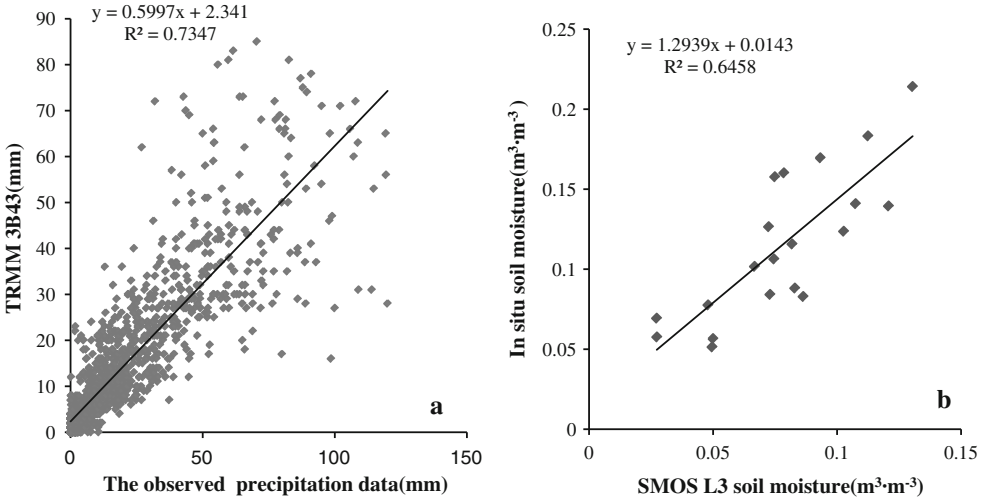

Fig. 2 **a** Scatter diagram between monthly precipitation derived from TRMM 3B43 and in situ precipitation. **b** Scatter diagram between monthly surface soil moisture derived from SMOS L3 and in situ surface soil moisture

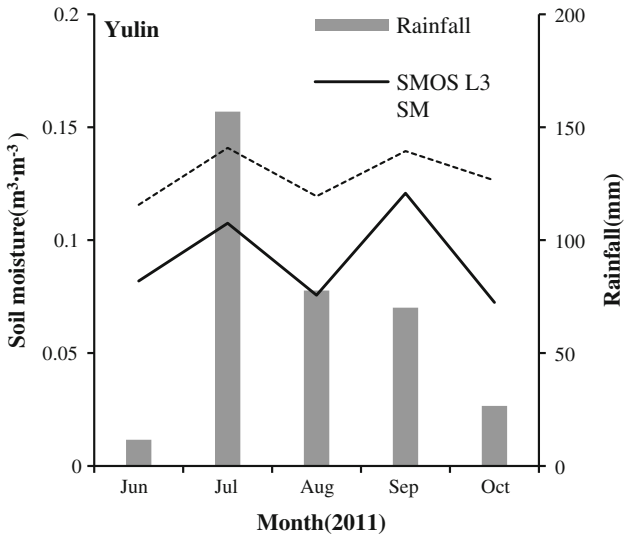

Fig. 3 Comparison between satellite data and ground measurements over the Yulin

Spatial and temporal stability analyses of NDVI, precipitation, ET and SSM

If a region exhibits time and spatial stable characteristics in precipitation, the RMSE δ of precipitation will be low in the whole region. Figure 5a shows the time stability characteristics RMSE δ_t of precipitation distributed from the smallest to largest over the Loess Plateau. Locations having low precipitation RMSE δ_t (red colors) have smaller seasonal changes. Locations with high precipitation RMSE δ_t (blue colors) correspond to zones where precipitation are often concentrated in 1 or 2 months from June to November. The distribution of precipitation spatial RMSE δ_s in Fig. 5b illustrates that the regions with low values (red colors) have similar precipitation amounts with spatially averaged conditions. The regions have high precipitation RMSE δ_s (blue colors) which depict zones with large difference in precipitation with spatially averaged conditions and correspond to the most humid area in the most eastern and most southern parts of the Loess Plateau and arid area in the most northern part of the Loess Plateau.

The ecosystem response to precipitation and soil moisture conditions can be discerned through spatial and temporal persistence of the NDVI fields (Mendez-Barroso et al. 2009). The temporal NDVI RMSE δ_t (Fig. 5c) supports to distinguish locations that closely track the temporal mean in each pixel. Regions with low NDVI RMSE δ_t (red colors) have relatively small changes in time and correspond to desert vegetation and farmland, which could be harvested two times per year or three times every 2 years. Desert vegetation has the lowest NDVI values in the region. These farmlands remain green during longer time periods. Regions with low spatial NDVI RMSE δ_s (Fig. 5d, red color) correspond to zones that closely track the spatially averaged conditions. These areas occupy large regional extents and coincide well with the location of locust wood, poplar wood, meadow steppe and farmland in which the planting system brings in one harvest a year. The regions have high NDVI RMSE δ_s (blue colors) which depict zones behaving differently from the spatial mean.

High ET temporal RMSE δ_t (Fig. 5e, blue color) is located in arid regions in the most northern part of the Loess Plateau and semi-humid regions in the southeast of the Loess Plateau. High ET temporal RMSE δ_t indicate that ecosystems have large evapotranspiration changes during the growing season. The loess hilly area of the Western Loess Plateau has low ET RMSE δ_t (red color), depicting that these regions have relatively small changes of evapotranspiration over time. Figure 5f presents the regions with high ET RMSE δ_s (blue color) which have large differences with the spatial mean.

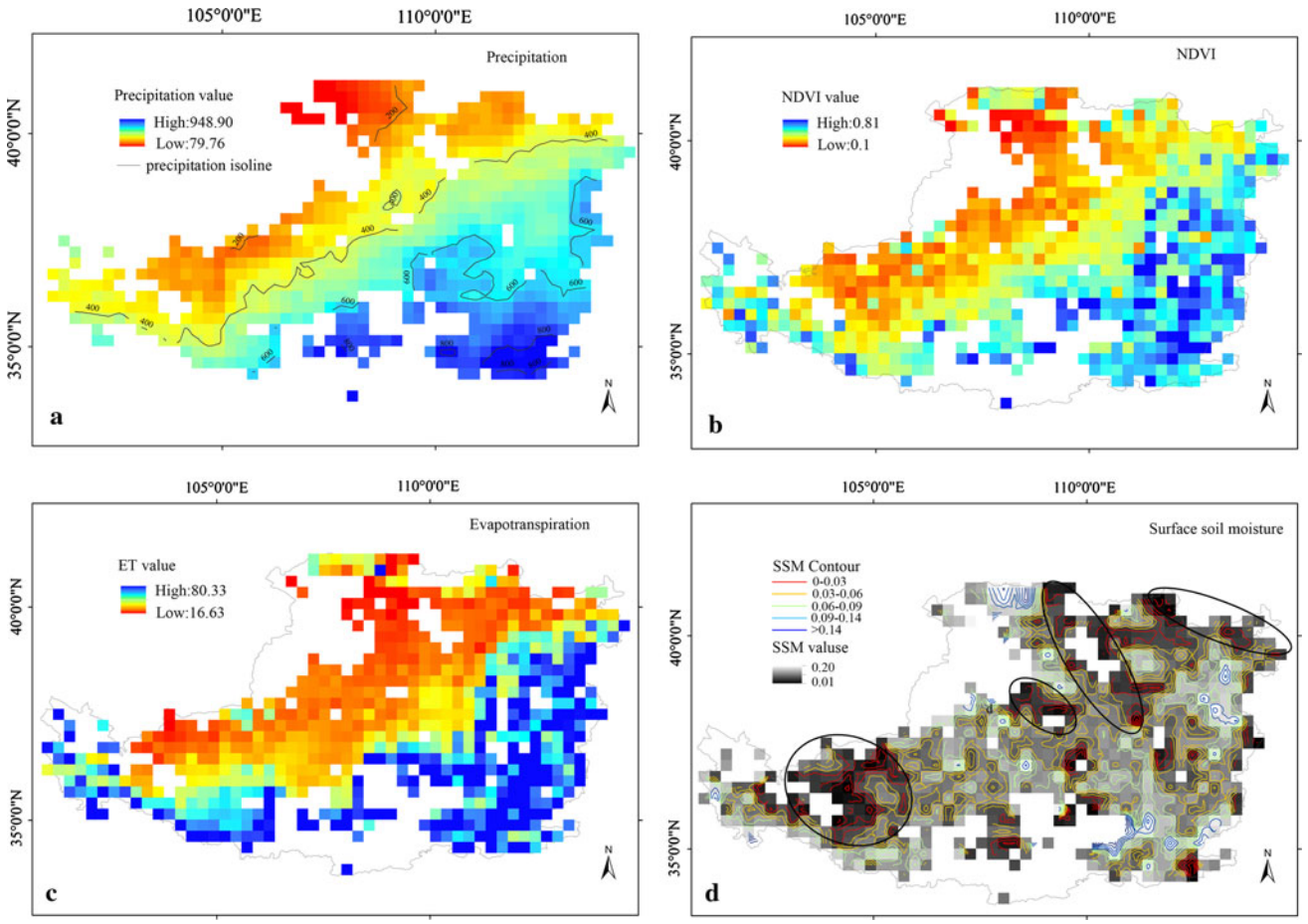

Fig. 4 Spatial distribution pattern of SSM, ET, precipitation and NDVI

The temporal RMSE δ_t of SSM are shown in Fig. 5g. The most northern part of the Loess Plateau has low SSM RMSE δ_t (red color), which indicates that SSM of this region is relatively stable during the growing season. The loess hilly areas of the Western Loess Plateau with high SSM RMSE δ_t (blue color) have large changes in SSM. High SSM spatial RMSE δ_s (Fig. 5h, blue color) is used to distinguish locations that have large differences with the spatial mean. In these pixels, the SSM is higher than in other regions.

The relation between temporal stability of SSM and NDVI, precipitation and ET in different soil moisture regime

To explore the relation between the temporal variability of SSM and NDVI, precipitation and ET, Table 1 presents the correlation between temporal RMSE δ_t of SSM and other RMSE δ_t in different soil moisture regime. The distribution of average SSM was well described by the skewed normal distribution. Using the standard deviation classification method, average SSM during the growing season was distributed into five classes. In Table 1, one can see that the impact of the temporal stability of NDVI, precipitation, ET on the temporal stability of SSM depends as follows on the soil moisture regime:

1. Dry surface soil moisture regime ($0 < \theta < 0.03$)
   Under this surface soil moisture condition, evapotranspiration temporal persistence has a higher positive correlation with surface soil moisture temporal persistence. Regions with high evapotranspiration seasonal changes have more surface soil moisture changes over time. Evapotranspiration is very sensitive to surface soil moisture and strongly controlled by soil moisture. Soil moisture provides a first-order control on land–atmosphere exchanges in soil moisture-limited regimes. ET is controlled mainly by soil water in arid areas and varies significantly according to the vegetation (cover and species) on the Loess Plateau (Fan et al. 2012).
2. Transitional surface soil moisture regime ($0.03 < \theta < 0.14$)
   Under this surface soil moisture value from 0.03 ($m^3\ m^{-3}$) to 0.06 ($m^3\ m^{-3}$), surface soil moisture temporal persistence has a positive correlation with precipitation temporal persistence. Under the surface

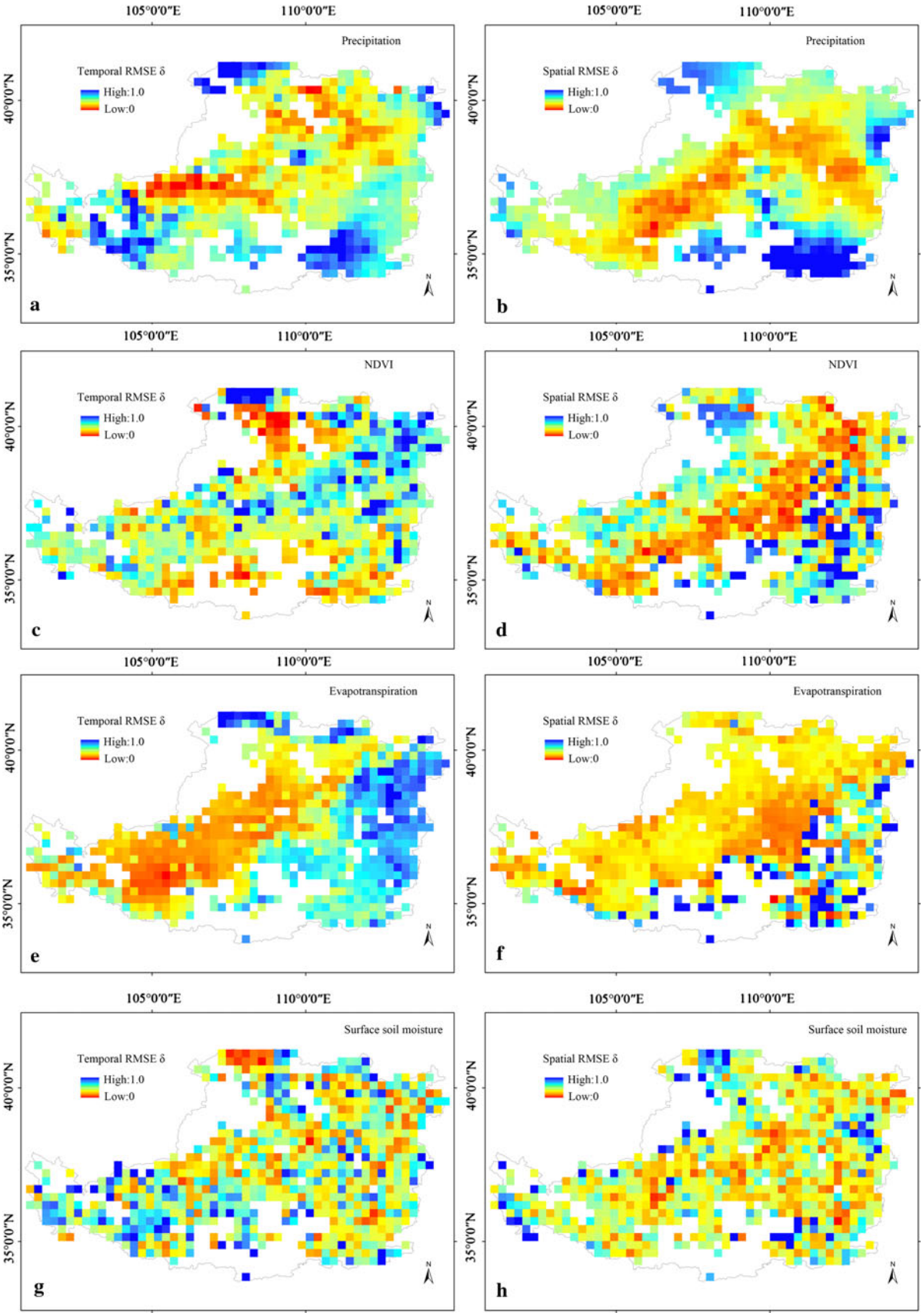

Fig. 5 Temporal and spatial RMSE of SSM, ET, precipitation and NDVI on the Loess Plateau

soil moisture with higher value, surface soil moisture temporal persistence has a negative correlation with vegetation temporal persistence and evapotranspiration temporal persistence. Under this class, soil moisture is central in the water exchange between soil, plants and the atmosphere.

3. Wet surface soil moisture regime ($\theta > 0.14$)
   Under this surface soil moisture condition, surface soil moisture temporal persistence has a higher negative correlation with evapotranspiration temporal persistence. Regions with large seasonal variation of surface soil moisture have low seasonal changes in evapotranspiration. In this region, high precipitation leads to high soil moisture which is closer to its maximum threshold (saturation). The soil moisture storage cannot be damped by vegetation water use.

The relation between SSM and precipitation, NDVI and ET in different climatic regions

The relation between surface soil moisture and precipitation, and NDVI in each pixel is explored using Pearson CCs. Table 2 reveals that the SSM and precipitation, NDVI and ET showed no significant correlation in arid regions on the Loess Plateau. This means that they are not the main factors impacting surface soil moisture in arid regions on the Loess Plateau.

Table 1 The correlation between temporal RMSE δ_t of SSM and other RMSE δ_t in different soil moisture regime

Surface soil moisture class	Surface soil moisture θ (m^3 m^{-3})	Factor	Pearson correlation
Dry	0–0.03	Evapotranspiration	0.537**
	0.03–0.06	Precipitation	0.169*
Transitional	0.06–0.09	NDVI and evapotranspiration	−0.197*, −0.135*
	0.09–0.14	Evapotranspiration	−0.171*
Wet	>0.14	Evapotranspiration	−0.621**

** Correlation is significant at the 0.01 level (2-tailed)

* Correlation is significant at the 0.05 level (2-tailed)

Table 2 The correlation coefficients between monthly SSM and precipitation, NDVI and ET in different climatic regions

		SSM	Precipitation	NDVI	ET
Arid					
SSM	Pearson correlation	1			
Precipitation	Pearson correlation	−0.106	1		
NDVI	Pearson correlation	0.080	0.304**	1	
ET	Pearson correlation	0.028	0.498**	0.577**	1
Semi-arid					
SSM	Pearson correlation	1			
Precipitation	Pearson correlation	0.227**	1		
NDVI	Pearson correlation	0.091**	0.364**	1	
ET	Pearson correlation	0.109**	0.418**	0.557**	1
Semi-humid 1					
SSM	Pearson correlation	1			
Precipitation	Pearson correlation	0.328**	1		
NDVI	Pearson correlation	0.318**	0.490**	1	
ET	Pearson correlation	0.220**	0.534**	0.626**	1
Semi-humid 2					
SSM	Pearson correlation	1			
Precipitation	Pearson correlation	0.229**	1		
NDVI	Pearson correlation	0.101**	0.372**	1	
ET	Pearson correlation	−0.037	0.202**	0.590**	1

** Correlation is significant at the 0.01 level (2-tailed)

The precipitation and SSM showed significant positive correlation in semi-arid, semi-humid 1 and semi-humid 2 regions on the Loess Plateau, with a higher correlation coefficient than other factors. In plant–soil–atmosphere systems, the plants act as a pathway along which water travels from the soil around their root zones to the atmosphere (Wang et al. 2011). The NDVI and SSM have a weak correlation in the semi-arid and semi-humid 2 regions and relatively stronger correlation in the semi-humid 1 region. It indicates that NDVI is a key factor for SSM distribution in semi-humid 1 regions and not a key factor for SSM distribution in semi-arid and semi-humid 2 regions.

The ET and SSM were positively correlated in semi-arid and semi-humid 1, but not significantly correlated in semi-humid 2 regions. Based on this result, only in the transitional climatic regions ET is a key factor for SSM distribution. In semi-humid 2 regions, evapotranspiration is large, but not controlled by soil moisture; thus, soil moisture has little impact on evapotranspiration (Seneviratne et al. 2010). Evaporation in wet climates is not highly sensitive to soil moisture variations; also, precipitation should not be sensitive to them (Koster et al. 2004).

From the results we conclude that precipitation is the major factor impacting soil moisture compared with the other related factors at the regional scale (Yao et al. 2012). In the semi-humid 1 region, the surface soil moisture is more sensitive to precipitation, NDVI and ET than in other climatic regions. Only in transitional regions between dry and wet climates are both conditions met for strong soil moisture–climate coupling (Seneviratne et al. 2010).

Conclusions

Soil moisture reflects the balance of precipitation, runoff and ET and exhibited various types of pulse events (Wang et al. 2012b). Surface soil moisture is one of the crucial variables in hydrological processes, which influence the exchange of water and energy fluxes at the land surface–atmosphere interface (Wang and Qu 2009). To the authors' knowledge, however, the controls exerted by factors on seasonal surface soil moisture have not been studied on the Loess Plateau. Furthermore, the temporal and spatial variations of surface soil moisture during the growing season are not well understood. Quantifying these spatio-temporal variations in a regional scale is fundamental for assessing the degree of coupling between ecologic, hydrologic and atmospheric processes.

By relating the remotely sensed data sets, we identify the following characteristics of the regional SSM dynamics and their relation to precipitation, ET and NDVI:

1. The spatial distribution of SSM is consistent with the spatial distribution pattern of rainfall, ET and NDVI. The amount of precipitation, and the mean value of NDVI and ET during the growing season decrease gradually from southeast to northwest. The spatial distribution pattern of SSM keeps with this trend.
2. The correlation between temporal RMSE δ_t of SSM and other RMSE δ_t indicates that ET is the largest factor for SSM temporal changes under dry surface soil moisture regime. Under wet surface soil moisture regime, the relations between the temporal variability of SSM and the temporal changes of other factors are not observed using simple metrics.
3. The impact of precipitation, ET and NDVI on SSM differed according to climatic region: in the arid region, there was no significant effect; in the semi-arid region, the effect of precipitation was significant; and in the semi-humid region, the effect of precipitation, ET and NDVI were significantly higher than that in the semi-arid region. Correlation analysis indicates a moderate degree of coupling between SSM and precipitation in most areas of the Loess Plateau. The precipitation was the major factor impacting the distribution of surface soil moisture compared with the other factors at the regional scale. However, under wet surface soil moisture regime, runoff has a major impact on the surface soil moisture, as in the situation in the most northern part of the Loess Plateau.

Acknowledgments This study was funded by the Natural Science Foundation of Gansu Province (No.1208RJYA063) and the "12th Five-Year Plan" national science and technology support program "The ecological restoration technology integration and experiment demonstration of degraded forests—the grassland in Loess hilly area" (No. 2011BAC07B04). The authors are grateful to the reviews for their helpful comments and suggestions to improve this manuscript.

References

Anderson LO, Malhi Y, Aragao LEOC et al (2010) Remote sensing detection of droughts in Amazonian forest canopies. New Phytol 187(3):733–750

Banks CJ, Gommenginger CP, Srokosz MA et al (2012) Validating SMOS ocean surface salinity in the Atlantic with argo and operational ocean model data. IEEE Trans Geosci Remote Sens 50(5):1688–1702

Berthon L, Mialon A, Cabot F et al (2012) Catds level 3 data product description. CESBIO, Toulouse

Bi HX, Li XY, Liu X et al (2009) A case study of spatial heterogeneity of soil moisture in the Loess Plateau, western China: a geostatistical approach. Int J Sedim Res 24(1):63–73

Bircher S, Balling JE, Skou N et al (2012) Validation of SMOS brightness temperatures during the HOBE airborne campaign, Western Denmark. IEEE Trans Geosci Remote Sens 50(5): 1468–1482

Bowler J, Chen K, Yuan B (1987) Systematic variations in loess source areas: evidence from Qaidan and Qinghai basins, west China. In: Liu TS (ed) Aspects of Loess research. China Ocean Press, Beijing, pp 164–174

Chen HS, Zhang W, Wang KL et al (2010) Soil moisture dynamics under different land uses on karst hillslope in northwest Guangxi. China Environ Earth Sci 61(6):1105–1111

Dente L, Su ZB, Wen J (2012) Validation of SMOS soil moisture products over the Maqu and Twente regions. Sensors 12(8): 9965–9986

D'Odorico P, Caylor K, Okin GS et al (2007) On soil moisture—vegetation feedbacks and their possible effects on the dynamics of dryland ecosystems. J Geophys Res Biogeosci 112:G04010. doi:10.1029/2006JG000379

Fan J, Jones SB, Qi LB et al (2012) Effects of precipitation pulses on water and carbon dioxide fluxes in two semiarid ecosystems: measurement and modeling. Environ Earth Sci 67(8):2315–2324

Fleming K, Awange JL, Kuhn M et al (2011) Evaluating the TRMM 3B43 monthly precipitation product using gridded rain gauge data over Australia. Aust Meteorol Ocean 61(3):171–184

Flores AN, Ivanov VY, Entekhabi D et al (2009) Impact of hillslope-scale organization of topography, soil moisture, soil temperature, and vegetation on modeling surface microwave radiation emission. IEEE Trans Geosci Remote Sens 47(8):2557–2571

Gherboudj I, Magagi R, Goita K et al (2012) Validation of SMOS data over agricultural and boreal forest areas in Canada. IEEE Trans Geosci Remote Sens 50(5):1623–1635

He X, Tang K, Zhang X (2004) Soil erosion dynamics on the Chinese Loess Plateau in the last 10,000 years. Mt Res Dev 24(4): 342–347

Islam T, Rico-Ramirez MA, Han DW et al (2012) Performance evaluation of the TRMM precipitation estimation using ground-based radars from the GPM validation network. J Atmos Sol-Terr Phys 77:194–208

Jackson TJ, Bindlish R, Cosh MH et al (2012) Validation of soil moisture and ocean salinity (SMOS) soil moisture over watershed networks in the US. IEEE Trans Geosci Remote Sens 50(5):1530–1543

Jacobs JM, Mohanty BP, Hsu EC et al (2004) SMEX02: field scale variability, time stability and similarity of soil moisture. Remote Sens Environ 92(4):436–446

Jia SF, Zhu WB, Lu AF et al (2011) A statistical spatial downscaling algorithm of TRMM precipitation based on NDVI and DEM in the Qaidam Basin of China. Remote Sens Environ 115(12): 3069–3079

Kerr YH, Waldteufel P, Wigneron JP et al (2001) Soil moisture retrieval from space: the Soil Moisture and Ocean Salinity (SMOS) mission. IEEE Trans Geosci Remote Sens 39(8):1729–1735

Kerr YH, Waldteufel P, Richaume P et al (2012) The SMOS soil moisture retrieval algorithm. IEEE Trans Geosci Remote Sens 50(5):1384–1403

Kim S (2012) Characterization of annual soil moisture response pattern on a hillslope in Bongsunsa Watershed, South Korea. J Hydrol 448:100–111

Kimura R, Shinoda M (2012) Estimation of surface soil water content from surface temperatures in dust source regions of Mongolia and China. Environ Earth Sci 65(6):1847–1853

Koster RD, Dirmeyer PA, Guo ZC et al (2004) Regions of strong coupling between soil moisture and precipitation. Science 305(5687):1138–1140

Kummerow C, Barnes W, Kozu T et al (1998) The tropical rainfall measuring mission (TRMM) sensor package. J Atmos Ocean Tech 15(3):809–817

Kummerow C, Simpson J, Thiele O et al (2000) The status of the Tropical Rainfall Measuring Mission (TRMM) after two years in orbit. J Appl Meteorol 39(12):1965–1982

Legates DR, Mahmood R, Levia DF et al (2011) Soil moisture: a central and unifying theme in physical geography. Prog Phys Geog 35(1):65–86

Li ZC, Wei ZG, Wang C et al (2012) Simulation and improvement of common land model on the bare soil of Loess Plateau underlying surface. Environ Earth Sci 66(4):1091–1097

Liu T (1985) Loess and the environment. China Ocean Press, Beijing

Liu XH, He BL, Li ZX et al (2011) Influence of land terracing on agricultural and ecological environment in the loess plateau regions of China. Environ Earth Sci 62(4):797–807

Mendez-Barroso LA, Vivoni ER, Watts CJ et al (2009) Seasonal and interannual relations between precipitation, surface soil moisture and vegetation dynamics in the North American monsoon region. J Hydrol 377(1–2):59–70

Mu Q, Heinsch FA, Zhao M et al (2007) Development of a global evapotranspiration algorithm based on MODIS and global meteorology data. Remote Sens Environ 111(4):519–536

Mu QZ, Jones LA, Kimball JS, et al (2009) Satellite assessment of land surface evapotranspiration for the pan-Arctic domain. Water Resour Res 45: W09420. doi:10.1029/2008WR007189

Mu QZ, Zhao MS, Running SW (2011) Improvements to a MODIS global terrestrial evapotranspiration algorithm. Remote Sens Environ 115(8):1781–1800

Njoku EG, Li L (1999) Retrieval of land surface parameters using passive microwave measurements at 6–18 GHz. IEEE Trans Geosci Remote Sens 37(1):79–93

Sanchez N, Martinez-Fernandez J, Scaini A et al (2012) Validation of the SMOS L2 soil moisture data in the REMEDHUS network (Spain). IEEE Trans Geosci Remote Sens 50(5):1602–1611

Seneviratne SI, Corti T, Davin EL et al (2010) Investigating soil moisture–climate interactions in a changing climate: a review. Earth Sci Rev 99(3–4):125–161

Shi H, Shao M (2000) Soil and water loss from the Loess Plateau in China. J Arid Environ 45(1):9–20

Srivastava PK, Han DW, Rico-Ramirez MA et al (2012) Selection of classification techniques for land use/land cover change investigation. Adv Space Res 50(9):1250–1265

Thakur JK, Srivastava P, Pratihast AK et al (2012a) Estimation of evapotranspiration from wetlands using geospatial and hydro-meteorological data, geospatial techniques for managing environmental resources. Springer, Heidelberg, pp 53–67

Thakur JK, Srivastava PK, Singh SK et al (2012b) Ecological monitoring of wetlands in semi-arid region of Konya closed Basin, Turkey. Reg Environ Change 12(1):133–144

Vivoni ER, Gebremichael M, Watts CJ et al (2008) Comparison of ground-based and remotely-sensed surface soil moisture estimates over complex terrain during SMEX04. Remote Sens Environ 112(2):314–325

Wang LL, Qu JJ (2009) Satellite remote sensing applications for surface soil moisture monitoring: a review. Frontiers Earth Sci China 3(2):237–247

Wang J, Fu BJ, Qiu Y et al (2001) Geostatistical analysis of soil moisture variability on Da Nangou catchment of the loess plateau. China Environ Geol 41(1–2):113–120

Wang J, Fu BJ, Qiu Y et al (2003) The effects of land use and its patterns on soil properties in a small catchment of the Loess Plateau. J Environ Sci 15(2):263–266

Wang YQ, Shao MA, Zhu YJ et al (2011) Impacts of land use and plant characteristics on dried soil layers in different climatic regions on the Loess Plateau of China. Agric For Meteorol 151(4):437–448

Wang L, D'Odorico P, Evans JP et al (2012a) Dryland ecohydrology and climate change: critical issues and technical advances. Hydrol Earth Syst Sci 16(8):2585–2603

Wang S, Fu BJ, Gao GY et al (2012b) Soil moisture and evapotranspiration of different land cover types in the Loess Plateau, China. Hydrol Earth Syst Sci 16(8):2883–2892

Xiong J, Mao DF, Yan NN (2009) Evaluation of TRMM satellite precipitation product in hydrologic simulations of Hai Basin. River Basin Res Plan Approach 180–186

Yao XL, Fu BJ, Lu YH et al (2012) The multi-scale spatial variance of soil moisture in the semi-arid Loess Plateau of China. J Soil Sediment 12(5):694–703

Zakharova E, Calvet JC, Lafont S et al (2012) Spatial and temporal variability of biophysical variables in southwestern France from airborne L-band radiometry. Hydrol Earth Syst Sci 16(6): 1725–1743

Zhang JT, Ru WM, Li B (2006) Relationships between vegetation and climate on the Loess Plateau in China. Folia Geobot 41(2): 151–163

Zhang T, Wen J, Su Z et al (2009) Soil moisture mapping over the Chinese Loess Plateau using ENVISAT/ASAR data. Adv Space Res 43(7):1111–1117

Zhao PP, Shao MA (2010) Soil water spatial distribution in dam farmland on the Loess Plateau, China. Acta Agric Scand Sect B-Soil Plant Sci 60(2):117–125

Zhou P, Wen AB, Zhang XB et al (2013) Soil conservation and sustainable eco-environment in the Loess Plateau of China. Environ Earth Sci 68(3):633–639

Zhu YJ, Shao MA (2008) Variability and pattern of surface moisture on a small-scale hillslope in Liudaogou catchment on the northern Loess Plateau of China. Geoderma 147(3–4):185–191